



The following Communications have been judged by at least two referees to be “very important papers” and will be published online at www.angewandte.org soon:

X. Xin, M. He, W. Han, J. Jung, Z. Lin*

Low-Cost Counter Electrodes for High-Efficiency Dye-Sensitized Solar Cells

J. Bacsá, F. Hanke, S. Hindley, R. Odra, G. R. Darling, A. C. Jones, A. Steiner*

The Solid-State Structures of Dimethylzinc and Diethylzinc

Z.-C. Wang, N. Dietl, R. Kretschmer, T. Weiske, M. Schlangen,* H. Schwarz*

Catalytic Redox Reactions in the CO/N₂O System Mediated by the Bimetallic Oxide-Cluster Couple AlVO₃⁺/AlVO₄⁺

C. D. N. Gomes, O. Jacquet, C. Villiers, P. Thuéry, M. Ephritikhine, T. Cantat*

A Diagonal Approach to Chemical Recycling of Carbon Dioxide: New Organocatalytic Transformation for the Reductive Functionalization of CO₂

X. Zhang, T. J. Emge, K. C. Hultsch*

A Chiral Phenoxyamine Magnesium Catalyst for the Enantioselective Hydroamination/Cyclization of Aminoalkenes and Intermolecular Hydroamination of Vinyl Arenes

M. A. Newton,* M. Di Michiel, A. Kubacka, A. Iglesias-Juez, M. Fernández-García*

Observing Oxygen Storage and Release at Work under Cycling Redox Conditions: Synergies between Noble Metal and Oxide Promoter

H. Qin, P. Gao, F. Wang, L. Zhao, J. Zhu, A. Wang, T. Zhang, R. Wu,* H. Zou*

Highly Efficient Extraction of Serum Peptides by Ordered Mesoporous Carbon



“If I won the lottery, I would be able to finally stop writing grants!”

In my opinion, the word “scientist” means explorer ...”

This and more about Michel R. Gagné can be found on page 11286.

Author Profile

Michel R. Gagné _____ 11286



C. R. Bertozzi



R. Metternich



J. A. Rogers

News

Kavli Lecturer:

C. R. Bertozzi _____ 11287

Head of Roche Research Group:

R. Metternich _____ 11287

Lemelson–MIT Prize:

J. A. Rogers _____ 11287

Obituaries

B. Feringa, B. Meijer _____ 11288

Hans Wynberg (1922–2011)

Books

Solvents and Solvent Effects in Organic Chemistry

Christian Reichardt, Thomas Welton

reviewed by R. Giernoth _____ 11289

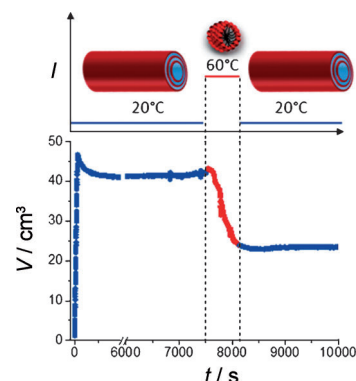
Highlights

Foams

A. Carl, R. von Klitzing* — 11290–11292

Smart Foams: New Perspectives Towards Responsive Composite Materials

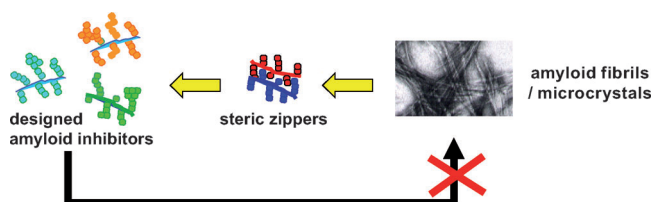
Hold the foam! Smart foams with a tunable surface-to-volume ratio have numerous potential applications, including decontamination. Recently fatty acid aggregates, the stability of which can be tuned by an external stimulus, were described. The picture shows a plot of the foam volume of a temperature-dependent foam which undergoes supramolecular reorganization.



Amyloid Inhibitors

A. Kapurniotu* — 11293–11294

Terminating the Amyloid Zipper by Design



Zip code: A potentially general, computational design approach has been used to devise peptide inhibitors of protein aggregation into amyloid fibrils. The atomic structures of “steric zippers”, which are formed by short fibril-forming

segments of the amyloidogenic proteins, serve as templates. The validity of the approach is demonstrated by the design of inhibitors of amyloid formation associated with Alzheimer's disease pathology and HIV infectivity.

Minireviews

Small-Molecule Probes

C. A. Olsen, A. S. Kristensen, K. Strømgaard* — 11296–11311

Small Molecules from Spiders Used as Chemical Probes



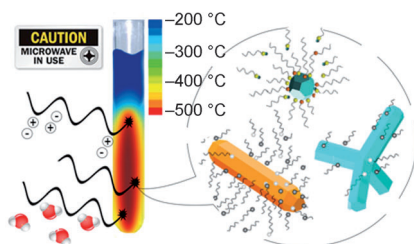
A tangled web: Semiochemicals and acylpolyamine toxins from spiders (see pictures) are unique biological probes and may even be considered potential thera-

peutic agents. In this Minireview a status update on the research regarding these interesting small molecules is presented.

For the USA and Canada: ANGEWANDTE CHEMIE International Edition (ISSN 1433-7851) is published weekly by Wiley-VCH, PO Box 191161, 69451 Weinheim, Germany. Air freight and mailing in the USA by Publications Expediting Inc., 200 Meacham Ave., Elmont, NY 11003. Periodicals

postage paid at Jamaica, NY 11431. US POSTMASTER: send address changes to *Angewandte Chemie*, Journal Customer Services, John Wiley & Sons Inc., 350 Main St., Malden, MA 02148-5020. Annual subscription price for institutions: US\$ 11,738/10,206 (valid for print and electronic / print or electronic delivery); for

individuals who are personal members of a national chemical society prices are available on request. Postage and handling charges included. All prices are subject to local VAT/sales tax.



If you can't stand the heat, get out of the kitchen: Direct volumetric and efficient heating by microwave irradiation enables the generation of colloidal nanocrystals in a fraction of the time required using conventional heating techniques (see picture). Among the advantages of this non-classical heating method is a great control of reaction temperature, allowing better versatility, reproducibility, and reduced processing times in the fabrication of high-quality nanocrystals.

Reviews

Microwave Chemistry

M. Baghbanzadeh, L. Carbone,
 P. D. Cozzoli,*
 C. O. Kappe* 11312–11359

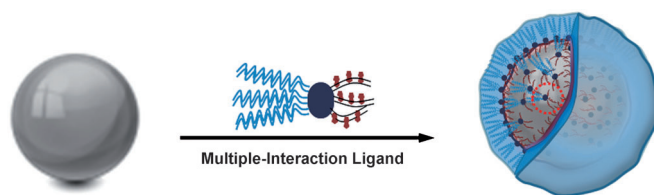
Microwave-Assisted Synthesis of Colloidal Inorganic Nanocrystals

Communications

Nanoparticles

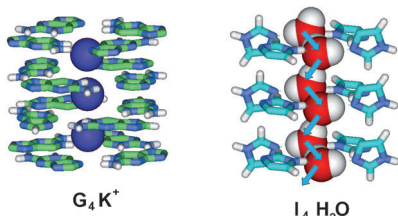
D. Ling, W. Park, Y. I. Park, N. Lee, F. Li,
 C. Song, S.-G. Yang, S. H. Choi, K. Na,*
 T. Hyeon* 11360–11365

Multiple-Interaction Ligands Inspired by Mussel Adhesive Protein: Synthesis of Highly Stable and Biocompatible Nanoparticles



All bound up: A poly(L-3,4-dihydroxyphenylalanine)-based ligand converts hydrophobic nanoparticles into hydrophilic and biocompatible species through several binding modes. Nanoparticles functionalized with this ligand (see picture) are

highly stable in various aqueous solutions. A successful in vivo MRI application using functionalized Fe_3O_4 nanoparticles confirmed their suitability for various biomedical applications.

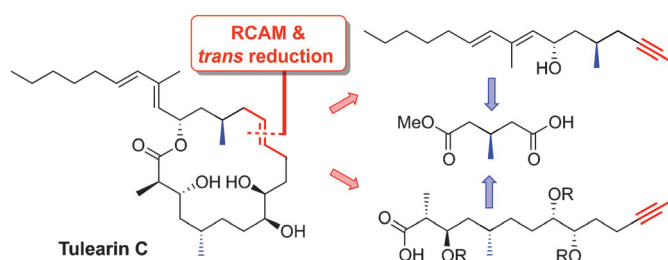


Dipolar water wires stabilize quartets of ureido imidazole compounds (I-quartets) in a manner reminiscent of stabilization of guanine (G) quartets by cation templating (see picture).

Water Channels

Y. Le Duc, M. Michau, A. Gilles, V. Gence,
 Y.-M. Legrand, A. van der Lee, S. Tingry,
 M. Barboiu* 11366–11372

Imidazole-Quartet Water and Proton Dipolar Channels



With the help of the smaller brother: Although alkyne metathesis will always be the little brother of alkene metathesis, it allows problems to be solved that are currently beyond reach of the more famous sibling. This notion is exemplified

by the tulearin macrolides, which could only be selectively forged by ring-closing alkyne metathesis (RCAM)/*trans* reduction using the latest generation of alkyne metathesis catalysts.

Natural Products

K. Lehr, R. Mariz, L. Leseurre, B. Gabor,
 A. Fürstner* 11373–11377

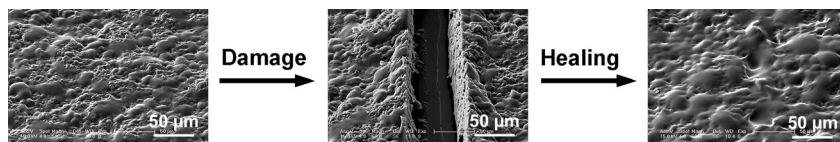
Total Synthesis of Tulearin C

Smart Materials

X. Wang, F. Liu, X. Zheng,
J. Sun* ————— 11378–11381



Water-Enabled Self-Healing of
Polyelectrolyte Multilayer Coatings



Heal thyself! Exponentially grown layer-by-layer-assembled polyelectrolyte multilayer coatings, which are mechanically robust under ambient conditions, can autonomically repair cuts several tens of

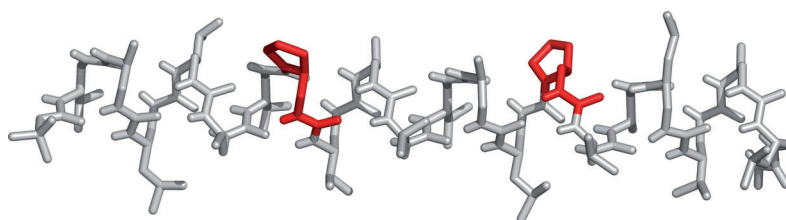
micrometers deep and wide when they are simply immersed in water or when water is sprayed on the coatings. The self-healing ability originates from the high flowability of these coatings in water.

Helical Structures

J. Fremaux, L. Fischer, T. Arbogast,
B. Kauffmann,
G. Guichard* ————— 11382–11385



Condensation Approach to Aliphatic
Oligoureia Foldamers: Helices with *N*-
(Pyrrolidin-2-ylmethyl)ureido Junctions



Caught in a fold: A simple and efficient coupling strategy to make aliphatic oligoureia foldamers is reported. Crystal structures show that the pyrrolidine units (red; see picture) do not impair the 2.5-helical folding of the oligoureias. This

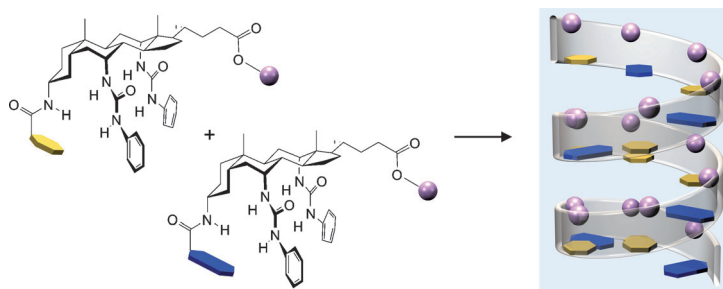
modular strategy enables assembly of long helical segments containing non-adjacent pyrrolidine units as exemplified by the synthesis of a helix that is approximately 40 Å long.

Crystal Engineering

R. Natarajan, G. Magro, L. N. Bridgland,
A. Sirikulkajorn, S. Narayanan, L. E. Ryan,
M. F. Haddow, A. G. Orpen,
J. P. H. Charmant, A. J. Hudson,
A. P. Davis* ————— 11386–11390



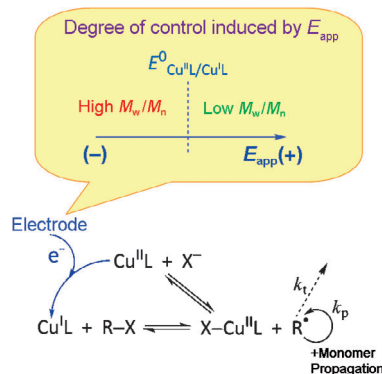
Nanoporous Organic Alloys



Crystal tuning: Organic molecules can be xenophobic, preferring to crystallize with their own kind. Though useful for purification, this precludes the tuning of crystal properties by doping or mixing. Nanoporous steroids provide an exception, as

their channels can accept a variety of termini (hexagons and spheres). The steroids can be cocrystallized in any ratio to give a wide range of chiral, potentially porous crystalline materials.

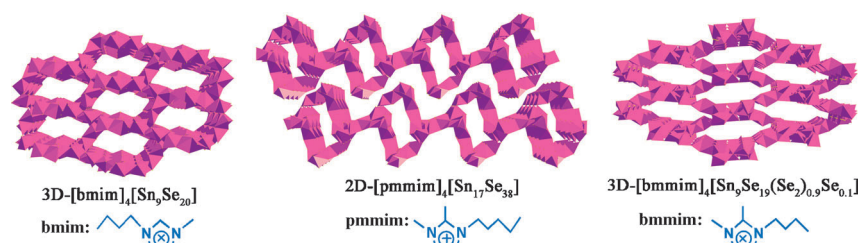
Enhanced control: Electrochemically mediated atom transfer radical polymerization (ATRP) allows easy modulation of the overall rate and control of polymerization through the variation of an external applied potential, E_{app} (see picture). This method has been successfully applied to aqueous ATRP of oligo(ethylene glycol) methyl ether methacrylate (OEOMA₄₇₅) catalyzed by Cu/tris(2-pyridylmethyl)-amine.



Atom Transfer Radical Polymerization

N. Bortolamei, A. A. Isse,
 A. J. D. Magenau, A. Gennaro,*
 K. Matyjaszewski* 11391–11394

Controlled Aqueous Atom Transfer
 Radical Polymerization with
 Electrochemical Generation of the Active
 Catalyst



Ready to direct: Crystalline selenidostannates were synthesized in imidazolium-based ionic liquids with a small amount of hydrazine monohydrate as additive (see

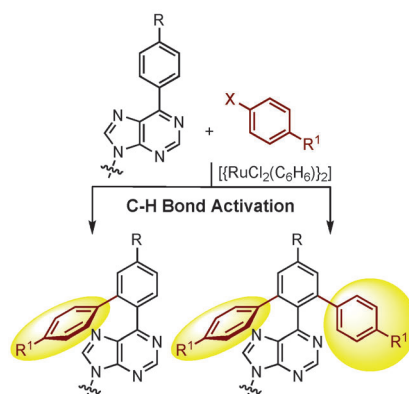
scheme). They are the first open-framework chalcogenides structurally directed by imidazolium cations and are inaccessible by traditional methods.

Ionic Liquids

J.-R. Li, Z.-L. Xie, X.-W. He, L.-H. Li,
 X.-Y. Huang* 11395–11399

Crystalline Open-Framework
 Selenidostannates Synthesized in Ionic
 Liquids

One aryl or two? The title reaction predominantly gives the monoarylation products with various amounts of diarylation product being observed in almost all cases (see scheme). Aryl iodides as well as aryl bromides were reactive under the optimized reaction conditions. The multiple nitrogen atoms in the purine, and oxygen atoms in the saccharide posed no problems in these transformations.

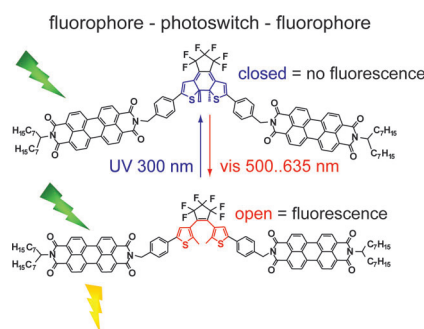


C–H Bond Activation

M. K. Lakshman,* A. C. Deb,
 R. R. Chamala, P. Pradhan,
 R. Pratap 11400–11404

Direct Arylation of 6-Phenylpurine and
 6-Arylpurine Nucleosides by Ruthenium-
 Catalyzed C–H Bond Activation

It takes three: The key functionalities of an optical transistor, gating and amplification, are demonstrated exploiting the photophysical properties of a molecular triad (see picture). Two building blocks of the triad are highly efficient fluorophores, whereas the third building block is a photochromic molecule that can be reversibly interconverted between two bistable forms by light.



Organic Optical Transistors

M. Pärss, C. C. Hofmann, K. Willinger,
 P. Bauer, M. Thelakkt,
 J. Köhler* 11405–11408

An Organic Optical Transistor Operated
 under Ambient Conditions

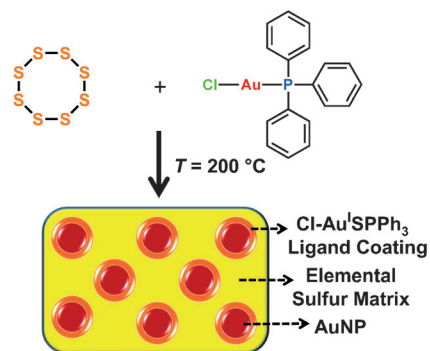
Sulfur Chemistry

W. J. Chung, A. G. Simmonds, J. J. Griebel, E. T. Kim, H. S. Suh, I.-B. Shim, R. S. Glass, D. A. Loy, P. Theato, Y.-E. Sung, K. Char, J. Pyun* **11409–11412**



Elemental Sulfur as a Reactive Medium for Gold Nanoparticles and Nanocomposite Materials

Get yellow: The utilization of elemental sulfur as an unconventional medium for the synthesis and stabilization of colloidal gold is reported. In this system, sulfur serves multiple functions to sulfurate PPh_3 , solubilize and reduce Au^{I} precursors into Au nanoparticles (NPs; see picture). Direct vulcanization of sulfur dispersions of AuNPs afforded cross-linked nanocomposites as confirmed by TEM, XRD, XPS, and Raman spectroscopy.

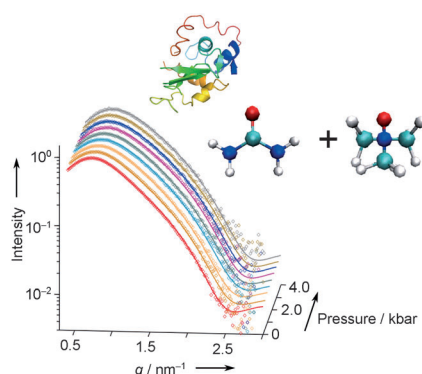


Proteins

M. A. Schroer, Y. Zhai, D. C. F. Wieland, C. J. Sahle, J. Nase, M. Paulus, M. Tolan, R. Winter* **11413–11416**



Exploring the Piezophilic Behavior of Natural Cosolvent Mixtures



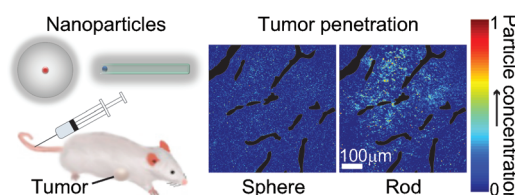
Marine organisms have evolved a surprising mechanism to counteract the deleterious effects of urea by trimethylammonium *N*-oxide (TMAO). The effect of pressure on the structure and intermolecular interactions of lysozyme in urea and TMAO solutions was studied (see picture). These findings help to understand the compensatory effect of urea–TMAO mixtures in deep-sea organisms.

Imaging Agents

V. P. Chauhan, Z. Popović, O. Chen, J. Cui, D. Fukumura, M. G. Bawendi,* R. K. Jain* **11417–11420**



Fluorescent Nanorods and Nanospheres for Real-Time In Vivo Probing of Nanoparticle Shape-Dependent Tumor Penetration



Shape dependent: Fluorescent quantum-dot-based nanospheres and nanorods with identical hydrodynamic size and surface properties but different aspect ratios were developed for real-time in vivo

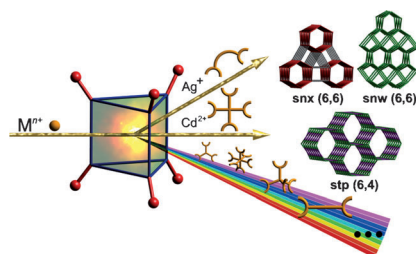
tumor imaging. The nanorods exhibited superior transport and distribution into mammary tumors in vivo versus nanospheres of similar plasma half-life.

Crystal Engineering

A. Schoedel, L. Wojtas, S. P. Kelley, R. D. Rogers, M. Eddaoudi, M. J. Zaworotko* **11421–11424**

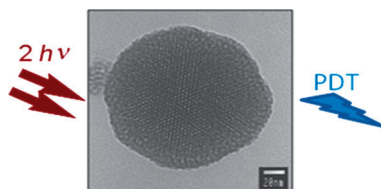


Network Diversity through Decoration of Trigonal-Prismatic Nodes: Two-Step Crystal Engineering of Cationic Metal–Organic Materials



MOMs the word! In a two-step process, first a trigonal-prismatic Primary Molecular Building Block ($[\text{Cr}_3\text{O}(\text{isonic})_6]^+$, tp-PMBB-1) was formed and then it was connected to linear linkers or square-planar nodes to afford three novel highly charged cationic metal–organic materials (MOMs) with **snx**, **snw**, and **stp** topologies.

Zap 'em! Multifunctionalized mesoporous silica nanoparticles induce significant reduction of tumor size upon two-photon excitation in the near-infrared region while being nontoxic under day-light illumination. These nanoparticles were further tested for in vivo two-photon photodynamic therapy (TPE-PDT). A 70% regression of tumor size after a single treatment was observed in athymic mice bearing tumor xenografts.

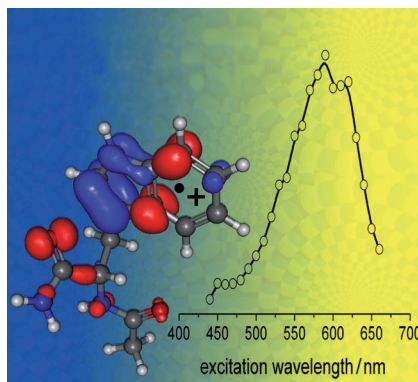


Photodynamic Therapy

M. Gary-Bobo, Y. Mir, C. Rouxel, D. Brevet, I. Basile, M. Maynadier, O. Vaillant, O. Mongin, M. Blanchard-Desce,* A. Morère, M. Garcia,* J.-O. Durand,* L. Raehm ————— **11425–11429**

Mannose-Functionalized Mesoporous Silica Nanoparticles for Efficient Two-Photon Photodynamic Therapy of Solid Tumors

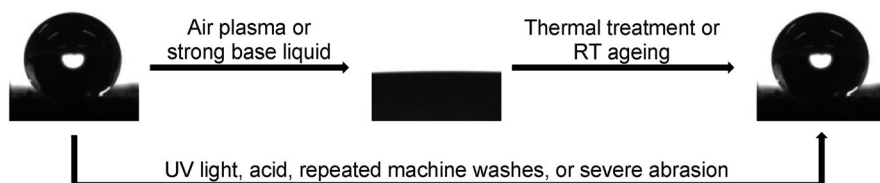
Mellow yellow: The canonical form of the tryptophan radical cation embedded in an isolated polypeptide shows a distinctive absorption in the yellow region of the spectrum, in contrast with the neutral radical form, which shows an absorption in the blue region (see picture). The spectroscopic diagnostic was supported by vibrational spectroscopy (IRMPD), time-dependent density functional theory, and multireference perturbation theory.



Protein Radicals

B. Bellina, I. Compagnon,* S. Houver, P. Maître, A.-R. Allouche, R. Antoine, P. Dugourd ————— **11430–11432**

Spectroscopic Signatures of Peptides Containing Tryptophan Radical Cations



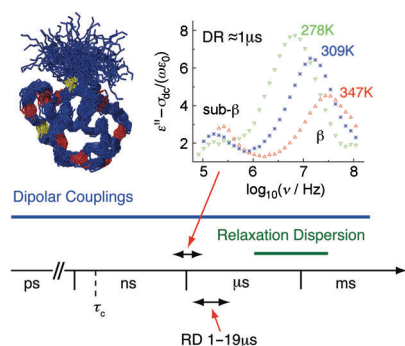
A fabric coating prepared from a homogeneous mixture of fluorinated-decyl polyhedral oligomeric silsesquioxane and hydrolyzed fluorinated alkyl silane shows remarkable self-healing superhydrophobic

and superoleophobic properties and excellent durability against UV light, acid, repeated machine washes, and severe abrasion (see picture).

Fabric Coatings

H. Wang, Y. Xue, J. Ding, L. Feng, X. Wang, T. Lin* ————— **11433–11436**

Durable, Self-Healing Superhydrophobic and Superoleophobic Surfaces from Fluorinated-Decyl Polyhedral Oligomeric Silsesquioxane and Hydrolyzed Fluorinated Alkyl Silane



A good combination: The lifetime of interconversion among the ground states of a protein ensemble representation could only be assigned to a time window that is four orders of magnitude large and ranges from 4 ns to 50 μs. By combining temperature-dependent NMR relaxation dispersion (RD) experiments and dielectric relaxation (DR) spectroscopy in solution, the lifetime was now identified to a value of $(10 \pm 9) \mu\text{s}$ at 309 K.

Protein Dynamics

D. Ban, M. Funk, R. Gulich, D. Egger, T. M. Sabo, K. F. A. Walter, R. B. Fenwick, K. Giller, F. Pichierri, B. L. de Groot, O. F. Lange, H. Grubmüller, X. Salvatella, M. Wolf, A. Loidl, R. Kree,* S. Becker, N.-A. Lakomek,* D. Lee,* P. Lunkenheimer,* C. Griesinger* ————— **11437–11440**

Kinetics of Conformational Sampling in Ubiquitin

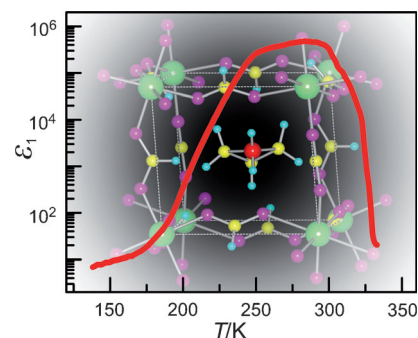
Dielectric Properties

B. Zhou, Y. Imai, A. Kobayashi,*
Z.-M. Wang,
H. Kobayashi* — 11441–11445



Giant Dielectric Anomaly of a Metal–Organic Perovskite with Four-Membered Ring Ammonium Cations

Pucker up: A metal–organic perovskite with four-membered-ring azetidinium cations (see structure) exhibited a very broad and unprecedentedly large dielectric peak near 280 K. It is highly possible that the ring-puckering instability of the four-membered-ring ammonium cation plays an essential role in inducing the change of the lattice symmetry and the extraordinarily large dielectric anomaly.

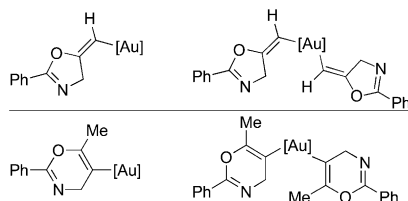


Reactive Intermediates

O. A. Egorova, H. Seo, Y. Kim, D. Moon,
Y. M. Rhee, K. H. Ahn* — 11446–11450



Characterization of Vinylgold Intermediates: Gold-Mediated Cyclization of Acetylenic Amides



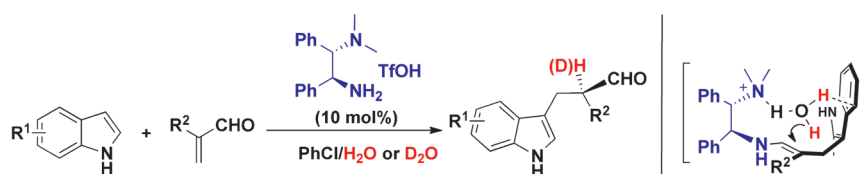
Hidden nuggets of gold: Mono- and divinylgold complexes (see scheme), key intermediates in the gold-mediated cyclization reaction of *N*-(propargyl)benzamides, are characterized by NMR and X-ray diffraction analyses. The monovinylgold intermediates undergo proto-de-auration in acetonitrile by the substrate. In aqueous media, they produce oxidized products. The divinylgold species undergo reductive elimination to produce the corresponding dimerized products.

Asymmetric Catalysis

N. Fu, L. Zhang, J. Li, S. Luo,*
J.-P. Cheng — 11451–11455



Chiral Primary Amine Catalyzed Enantioselective Protonation via an Enamine Intermediate



Enamine protonation: A chiral diamine catalyzes an asymmetric Friedel–Crafts reaction through catalytic enantioselective protonation of an enamine. This process can be applied to a range of α -substituted acroleins and indoles with high yields of

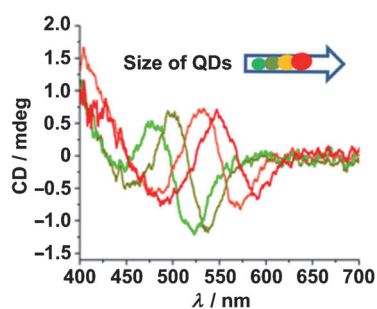
products and high enantioselectivity (up to 94% *ee*). An O–H/ π interaction between H_2O and the indole ring was found to play an important role in the transition state (see scheme).

Chiral Quantum Dots

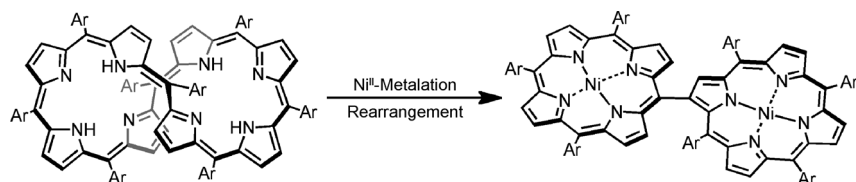
Y. Zhou, Z. Zhu, W. Huang, W. Liu, S. Wu,
X. Liu, Y. Gao, W. Zhang,*
Z. Tang* — 11456–11459



Optical Coupling Between Chiral Biomolecules and Semiconductor Nanoparticles: Size-Dependent Circular Dichroism Absorption



Sizing up QDs: CdTe or CdSe quantum dots (QDs) stabilized by chiral biomolecules show size-dependent circular dichroism (CD) characteristics in the visible light region. Theoretical calculations reveal that the origin of this CD is the combination of the weak optical activity of the biomolecules and the large enhancement effects from the strong absorption of QDs.



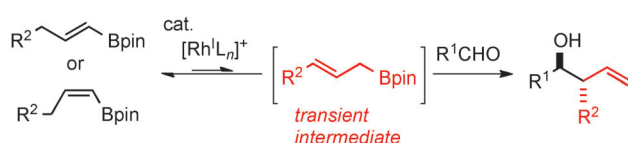
Breaking and entering: A figure-of-eight dinickel(II) complex and skeletal rearrangement products including a pyrrole-ring-cleaved product, a directly meso-β-linked diporphyrin (see scheme), and a

dearylative oxygenation product have been formed in moderate yields by a nickel(II) metalation of [36]octaphyrin(1.1.1.1.1.1.1.1) in acetonitrile.

Porphyrinoids

Y. Tanaka, H. Mori, T. Koide, H. Yorimitsu, N. Aratani, A. Osuka* — 11460–11464

Rearrangements of a [36]Octaphyrin Triggered by Nickel(II) Metalation: Metamorphosis to a Directly meso-β-Linked Diporphyrin



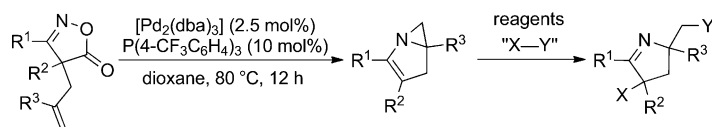
Synthetic equivalents: 1-Alkenylboronates perform the role of an allylating reagent. Their reaction with aldehydes in the presence of a cationic rhodium(I)/dppm

catalyst results in a highly diastereoselective production of *anti*-configured homoallylic alcohols (see scheme; Bpin = 4,4,5,5-tetramethyl-1,3,2-dioxaborolanyl).

Allylation Reactions

H. Shimizu, T. Igarashi, T. Miura, M. Murakami* — 11465–11469

Rhodium-Catalyzed Reaction of 1-Alkenylboronates with Aldehydes Leading to Allylation Products



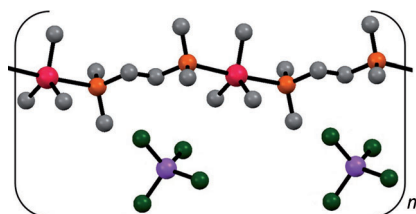
A decarboxylative intramolecular aziridination reaction of alkene-tethered 4H-isoxazol-5-ones with a palladium/phosphine catalyst gave 1-azabicyclo[3.1.0]hex-2-enes in moderate to high yields (see

scheme; dba = dibenzylideneacetone). The resulting N-fused bicyclic aziridines readily reacted with various reagents to afford ring-opening pyrroline derivatives.

Synthetic Methods

K. Okamoto, T. Oda, S. Kohigashi, K. Ohe* — 11470–11473

Palladium-Catalyzed Decarboxylative Intramolecular Aziridination from 4H-Isioxazol-5-ones Leading to 1-Azabicyclo[3.1.0]hex-2-enes



Rare examples of P–Sn bonded cations (see structure; purple Al, gray C, green Cl, orange P, red Sn) are formed in reactions of Me₃P or Me₂PCH₂CH₂PMe₂ with Me₃SnCl or *n*Bu₂SnCl₂ in the presence of a halide abstracting agent. The demonstrated versatility of the reactions, structures and bonding arrangements bodes well for the development of a diverse P–Sn chemistry by exploiting coordination chemistry for P–Sn bond formation.

Phosphorus–Tin Compounds

E. MacDonald, L. Doyle, N. Burford,* U. Werner-Zwanziger, A. Decken — 11474–11477

Stannylphosphonium Cations

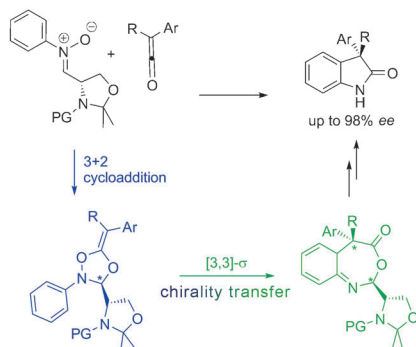


Pericyclic Cascades

N. Çelebi-Ölçüm, Y.-h. Lam, E. Richmond,
K. B. Ling, A. D. Smith,*
K. N. Houk* **11478–11482**



Pericyclic Cascade with Chirality Transfer:
Reaction Pathway and Origin of
Enantioselectivity of the Hetero-Claisen
Approach to Oxindoles



A new pericyclic cascade is proposed for the chiral auxiliary-controlled synthesis of 3,3-disubstituted oxindoles from nitrones and ketenes. The remarkable acyclic 1,6-stereochemical induction, hitherto unexplained, is rationalized by a stereoselective 3+2 cycloaddition step, which installs the stereochemistry, and a chirality transfer step facilitated by a hetero-[3,3]-sigmatropic rearrangement (see picture; PG = protecting group).

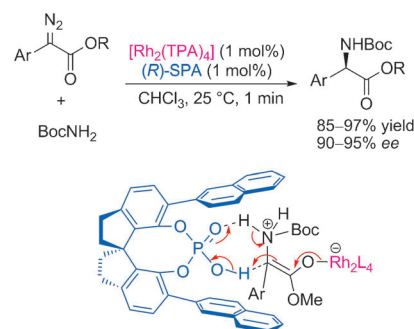
Asymmetric Catalysis

B. Xu, S.-F. Zhu,* X.-L. Xie, J.-J. Shen,
Q.-L. Zhou* **11483–11486**



Asymmetric N–H Insertion Reaction
Cooperatively Catalyzed by Rhodium and
Chiral Spiro Phosphoric Acids

So near so SPA: Achiral dirhodium(II) carboxylates and chiral spiro phosphoric acids (SPA) cooperatively catalyzed asymmetric N–H insertion reactions with high enantioselectivity, high yields, and fast reaction rates at low catalyst loading (see scheme; Boc = *tert*-butoxycarbonyl, TPA = triphenylacetyl). Chiral spiro phosphoric acid assisted asymmetric proton transfer is proposed as the chiral induction step.



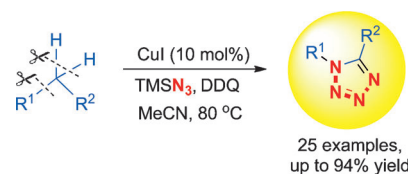
Nitrogen Heterocycles

F. Chen, C. Qin, Y. Cui,
N. Jiao* **11487–11491**



Implanting Nitrogen into Hydrocarbon
Molecules through C–H and C–C Bond
Cleavages: A Direct Approach to
Tetrazoles

From simple beginnings: A novel Cu-promoted direct incorporation of nitrogen into simple hydrocarbon molecules under mild and neutral reaction conditions is described. 1,5-Disubstituted tetrazoles are efficiently constructed by two C_{sp}³–H and one C–C bond cleavages (see scheme; TMS = trimethylsilyl). This protocol provides a new and unique strategy to functionalize simple and readily available hydrocarbon molecules.

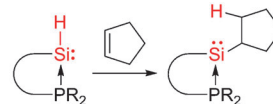
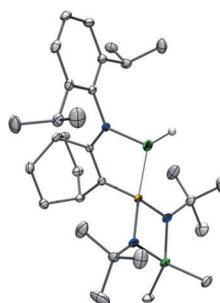


Hydrosilylation

R. Rodriguez, D. Gau, Y. Contie, T. Kato,*
N. Saffon-Merceron,
A. Baceiredo* **11492–11495**

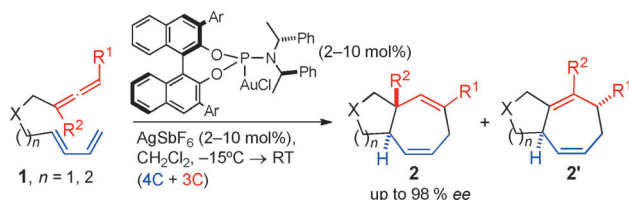


Synthesis of a Phosphine-Stabilized
Silicon(II) Hydride and Its Addition to
Olefins: A Catalyst-Free Hydrosilylation
Reaction



No cat.s allowed: A stable and isolable tricoordinate silicon(II) hydride stabilized by a phosphine ligand was successfully synthesized and fully characterized (see structure, Si green, P yellow, N blue,

C gray, H white). Interestingly, this silicon hydride adds to olefins in an unprecedented catalyst-free hydrosilylation reaction in very mild conditions.



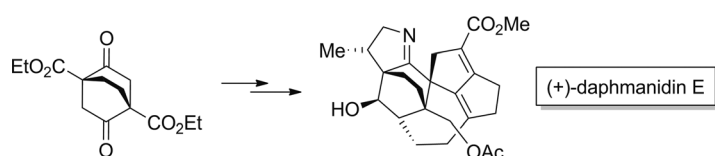
Allene-tethered dienes (1) undergo an intramolecular and highly enantioselective (4+3) cycloaddition when treated with suitable chiral phosphoramidite/gold(I) catalysts (see scheme; Ar = 9-

anthracenyl). The reactions provide synthetically relevant [5.3.0] and [5.4.0] fused bicyclic systems **2** with good yields, complete diastereocontrol, and excellent enantioselectivities.

Enantioselective Cycloaddition

I. Alonso, H. Faustino, F. López,*
 J. L. Mascareñas* 11496–11500

Enantioselective Gold(I)-Catalyzed Intramolecular (4+3) Cycloadditions of Allenedienes



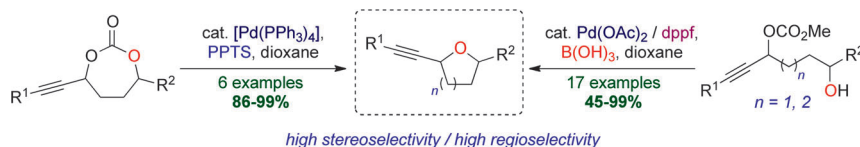
From ring to ring: The first total synthesis of (+)-daphmanidin E features rapid access to an enantiomerically pure bicyclo[2.2.2]octadione and elaboration around its periphery through the implementation of two Claisen rearrangements,

the use of a copper/peptide complex for reagent-controlled stereoselective conjugate addition, a diastereoselective hydroboration, and a cobalt-catalyzed alkyl-Heck cyclization.

Natural Products

M. E. Weiss,
 E. M. Carreira* 11501–11505

Total Synthesis of (+)-Daphmanidin E



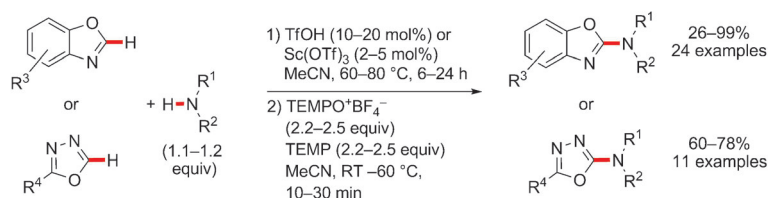
Oxyacetylene: Unusual palladium-catalyzed cyclizations of cyclic and acyclic propargylic carbonates give 2-alkynyl oxacycles. The reactions proceed with very high stereoselectivity for both *syn*- and *anti*-disubstituted furans and pyrans, and

with exceptional regioselectivity. In addition, two-directional cyclizations of bis-propargylic carbonate substrates yield bifurans with complete stereocontrol for all diastereomers.

Oxygen Heterocycles

D. S. B. Daniels, A. L. Thompson,
 E. A. Anderson* 11506–11510

Palladium-Catalyzed Asymmetric Synthesis of 2-Alkynyl Oxacycles



No transition metals are necessary to convert benzoxazoles and 1,3,4-oxadiazoles into the corresponding pharmacologically interesting 2-aminated heterocycles by formal direct C(2)-amination

using tetramethylpiperidine-*N*-oxoammonium tetrafluoroborate (TEMPO⁺BF₄[–]) as an oxidant (see scheme; TEMP = 2,2,6,6-tetramethylpiperidine; TfOH = trifluoromethanesulfonic acid).

C–H Amination

S. Wertz, S. Kodama,
 A. Studer* 11511–11515

Amination of Benzoxazoles and 1,3,4-Oxadiazoles Using 2,2,6,6-Tetramethylpiperidine-*N*-oxoammonium Tetrafluoroborate as an Organic Oxidant

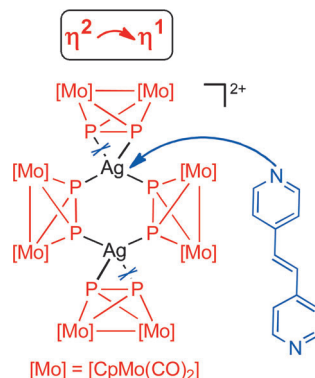


Hybrid Materials

B. Attenberger, S. Welsch, M. Zabel,
E. Peresyphina,
M. Scheer* ————— 11516–11519



Diphosphorus Complexes as Building
Blocks for the Design of Phosphorus-
Containing Organometallic–Organic
Hybrid Materials



The flexible coordination behavior of P_n ligand complexes in solution is utilized to create unprecedented coordination networks. In combination with ditopic organic linker units, organometallic–organic hybrid compounds are accessible. Depending on the nature of the metal center, metallaparacyclophane-like structures as well as 1D and 2D polymeric arrangements can be achieved.

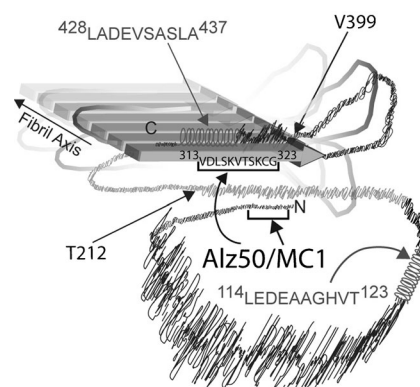
Alzheimer Research

S. Bibow, M. D. Mukrasch,
S. Chinnathambi, J. Biernat, C. Griesinger,
E. Mandelkow,
M. Zweckstetter* ————— 11520–11524



The Dynamic Structure of Filamentous
Tau

Getting inside a fuzzy coat: The dynamic structure of the “fuzzy coat”, N- and C-terminal sections around the core of the tau filament consists of over 200 amino acids, and has been characterized by NMR spectroscopy (see picture, model of the long range interactions). The results indicate how conformation specific antibodies bind to the tau protein (fibers of which are a characteristic symptom of Alzheimer disease).

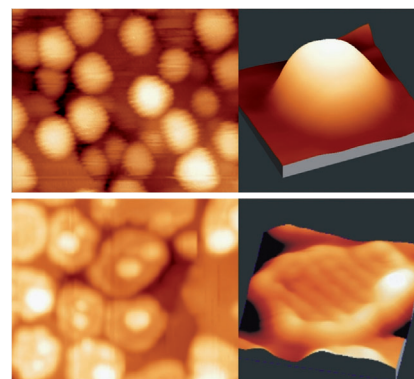


Doping

X. Shao, S. Prada, L. Giordano,*
G. Pacchioni, N. Nilius,*
H.-J. Freund ————— 11525–11527

Tailoring the Shape of Metal Ad-Particles
by Doping the Oxide Support

Just a Mo: Tiny Mo concentrations in a CaO film can influence the growth of adsorbed gold. On undoped films, three dimensional gold structures form (see picture, top) whereas on the doped films flat islands appear (bottom). The change results from a charge transfer from the Mo dopant to the Au atoms, a process suggested by STM measurements and DFT calculations.



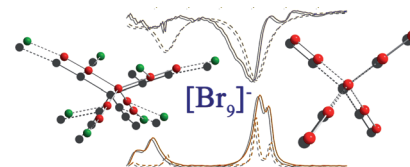
Polybromides

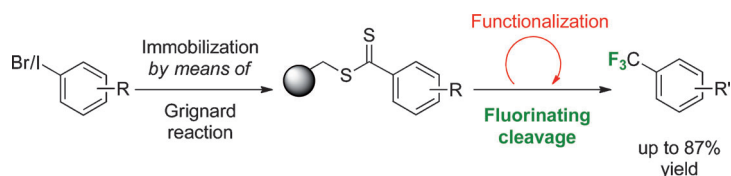
H. Haller, M. Ellwanger, A. Higelin,
S. Riedel* ————— 11528–11532



Structural Proof for a Higher Polybromide
Monoanion: Investigation of
[N(C₃H₇)₄][Br₉]

Bromine's nine: The first crystal structure of a higher polybromide monoanion, [NPr₄][Br₉] is reported along with its IR and Raman spectra (see picture). Owing to its low melting point and vapor pressure, this substance can be classified as an ionic liquid. It shows surprisingly high conductivity which may enable its applications as electrolyte in batteries.





Save the best for last: In the first method for the trifluoromethylation of immobilized arenes, the aryl halides are attached through a dithioester linkage to the Merrifield resin and then functionalized by means of numerous reactions including

transition-metal-catalyzed cross-couplings. In the final step the fluorinating cleavage reaction provides the trifluoromethylarenes in good yields and high purities.

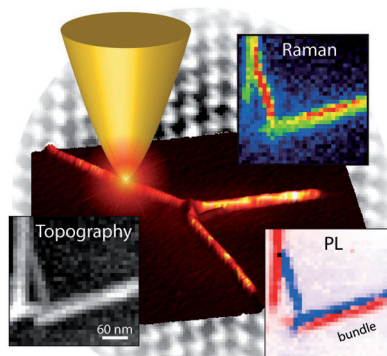
Trifluoromethylation

M. Döbele, M. S. Wiehn,
S. Bräse* ————— 11533–11535

Traceless Solid-Phase Synthesis of
Trifluoromethylarenes



Down to the wire: High-resolution photoluminescence (PL) and Raman images of CdSe nanowires were obtained using tip-enhanced near-field optical microscopy. They show that the optical properties of the CdSe nanowires vary significantly within a few nanometers leading to strong spatial fluctuations in both PL intensities and energies (see picture).



Nanomaterials

M. Böhmler, Z. Wang, A. Myalitsin,
A. Mews, A. Hartschuh* — 11536–11538

Optical Imaging of CdSe Nanowires with
Nanoscale Resolution



Supporting information is available
on www.angewandte.org
(see article for access details).



A video clip is available as Supporting
Information on www.angewandte.org
(see article for access details).



This article is available
online free of charge
(Open Access)

Looking for outstanding employees?

Do you need another expert for your excellent team?
... Chemists, PhD Students, Managers, Professors, Sales Representatives...

Place an advert in the printed version and have it made available online for
1 month, free of charge!

Angewandte Chemie International Edition

Advertising Sales Department: Marion Schulz

Phone: 0 62 01 - 60 65 65

Fax: 0 62 01 - 60 65 50

E-Mail: MSchulz@wiley-vch.de

Service

**Spotlight on Angewandte's
Sister Journals** ————— 11 282–11 284

Vacancies ————— 11 285

Preview ————— 11 539